History effect on squeal with a mesoscopic approach to friction materials

Vincent Magnier, D. Naidoo Ramasami, J.F. Brunel, P. Dufrénoy, T. Chancelier

History effect on squeal with a mesoscopic approach to friction materials

V. Magnier[a,b,c,*], D. Naidoo Ramasami[a,b,c], J.F. Brunel[a,b,c], P. Dufrénoy[a,b,c], T. Chancelier[d]

[a] *Université Lille Nord de France, F-59000 Lille, France*
[b] *Lille1-LML, F-59655 Villeneuve d'Ascq, France*
[c] *CNRS, UMR 8107, F-59655 Villeneuve d'Ascq, France*
[d] *Chassis Brake International, France*

Abstract

Friction pads are made by a recipe of numerous components leading to a heterogeneous material. The originality of this paper is firstly to propose a method leading to identify local mechanical properties of friction a pad, performed at different locations, via an indentation test. Secondly, the mechanical properties obtained for each location are introduced in a modeling to perform a complex modal analysis. A comparison with an equivalent homogeneous friction pad is performed to highlight the difference. Finally, the previous approach is extended to other friction pads which have been submitted to the same test sequence but interrupted at different times to investigate the history effect.

Keywords: Heterogeneity properties, Indentation tests, Squeal, History effect.

1. Introduction

From the very first brake lining in the early 20^{th} century to the common brake pad known today, several breakthroughs have been performed to improve performance such as power dissipation, recovery, pedal feel, durability, weight, etc. However, one of the top issue automotive industry encounters is noise. Indeed, the contact interface between the disc and the pad generates

*Corresponding author. Tel: +33 (0)3 28 76 73 57
Email address: `vincent.magnier@polytech-lille.fr` (V. Magnier)

numerous kinds of high-pitched noises and, even if it does not significantly affect performances, the consequence is very high customer complaints warranty cost each year. This is a high-pitched noise between 1 and 10 kHz up to 120dB. In order to reduce this noise and to identify the source and the mechanisms attached, it is necessary to take a look at the full process of supplying a classic disc brake system.

In the literature review, it has been seen that squeal noise occurrence is commonly linked to mode lock-in between components of the braking system : braking pads, disc, caliper etc. This method is one relevant way to understand squeal.

First, it is well-assumed that contact geometry at a global scale has an important impact on squeal noise occurrence and so mode lock-in between pad and disc. Furthermore, many studies have shown a dependency of pad geometry into this coupling. In [6], it is shown that chamfered or cut-off pad geometry modulates occurrence and frequency of squeal, or more recently in [11], that the pad length also impacts these results. But, in smaller geometry scales, the contact geometry influences also the mode lock-in. Thus, [2] defines five scales for considering the contact interface. They all take into account the dynamic and physical transformation of materials.

An interesting approach is the work achieved in [13]. By measuring the brake lining, the authors proposed to investigate the micro-mechanical properties of the surfaces using indentation tests. The goal is to model the effect of roughness [26], which can be determined like [7], and other non-linearities of the contact interface. In [1] the authors have included in their numerical model a non-uniform distribution of the contact pressure from experimental static measurements. Furthermore, they have enhanced their model taking into account the wear of the material. They thus obtained good correlation between the experimental and the numerical in terms of wear of the contact and contact distribution. Similarly, the complex modal analysis performed with various distributions of pressure instabilities shows similar results obtained experimentally.

Through these kinds of work, surface profile effect can be easily modeled. However, the literature shows the lacks of understanding and identification of mechanical behavior of the tribo-layer. There is almost any real complete multi-scale approach from the system to the contact interface. These are mostly simple approaches and only a few finite elements approaches except for example Heussaff work [13], which is only focused on the surface interface. The goal would be to take also into account the near-contact volumic

properties including surface and material heterogeneous properties.
In the finite element modal analysis, many studies have been conducted in academic and industrial R& D as in [20], [15], [5], [25], [4], [27] and [21]. The list presented here is not exhaustive. Complete brake models with a large number of degrees-of-freedom are of interest in these works. It seems relevant to have a complete model to compare for example with experimental data, but the complexity remains in the modeling of bounding between components, as contact interface and on material properties near the contact surface. In fact it is clear that changes in the friction material occur during braking, in a non-uniform manner at different location, as well as the evolution of the contact interface.
So in this paper, the first step focuses on the characterization of the "local" equivalent mechanical properties. Indeed, the friction pad is divided into 140 square areas (called "patches") and an indentation test on each patch is performed to have the hardness. From this data for each patch, an inverse numerical method is performed to identify mechanical properties. This protocol is repeated for four friction pads which have been submitted different braking histories. After the second step consists, with an implementation of the different local properties in a global friction pad, to a complete complex eigenvalue analysis of a braking system in order to draw attention to the parameter on mode lock-in which is the most critical. A comparison between these heterogeneous friction pads and an equivalent homogeneous (which is the main assumption for the major work on brake squeal) is performed.

2. Indentation test

2.1. Motivation

In general, the lining materials of automotive brakes are usually composites manufactured by compaction of coarse powders including many different components (typically 20 to 30). The mechanical properties of the components span a wide range, from very soft and easily worn phenolic resins to hard and wear resistant fibres and abrasive particles. Types and relative amounts of ingredients have been determined by empirical observations including a binder resin, reinforcing fibers, solid lubricants, abrasives, fillers and friction modifiers. So, the friction pad is a highly heterogeneous material whose properties are difficult to determine at a local scale. Here, the chosen solution in order to obtain a mesoscopic information is indentation testing performed on the complete friction pad. The methodology to evaluate mechanical properties at this scale is described in the following.

2.2. Protocol of the indentation test

The 10mm Brinell indenter shape has been chosen. The choice of the Brinell test is motivated by a smooth contact between pad and indenter hoping to work in the elastic domain. Indeed, the friction pad has a crumbly composition and it is necessary to no damage the material in order to identify the elastic properties. Moreover, a large radius is desirable and a ball geometry of diameter 10mm is a good compromise with the size of raw materials which can be milimetric.
All indentation tests for this study are performed with 2.5 ZHU Zwick device with the following test parameters:

- Maximum load : 300N
- Load and unload speed : 10N.s^{-1}
- Dwell time at the maximum load: 15s

The choice of these different parameters is deeply explained in [22]. Some typical load-displacement curves are illustrated in figure 1. The different curves show a wide dispersion of results depending on the test location, illustrating the heterogeneous behavior of the friction material.

2.3. Preliminary works

In this part, a mapping of the pad is done to perform indentation test on each cell. Even if the volume affected by the indentation test (called "patch" later) is heterogeneous, the behavior is homogenized and it is considered in the following as homogeneous on each patch.
To define the mapping pad, the patch size must be defined. For that, a numerical model of the indentation has been done to identified the affected volume for realistic test conditions (see fig 2). The finite element mesh size near the contact is equal to 0.01mm. For the contact, the Lagrangian method is used and a coefficient of friction of 0.4 is considered. With the geometry and loading conditions previously described and a macroscopic Young modulus of 3000 MPa, the size (radius) of the affected volume has been evaluated and a patch size of $\phi = 0.925mm$ has been defined.

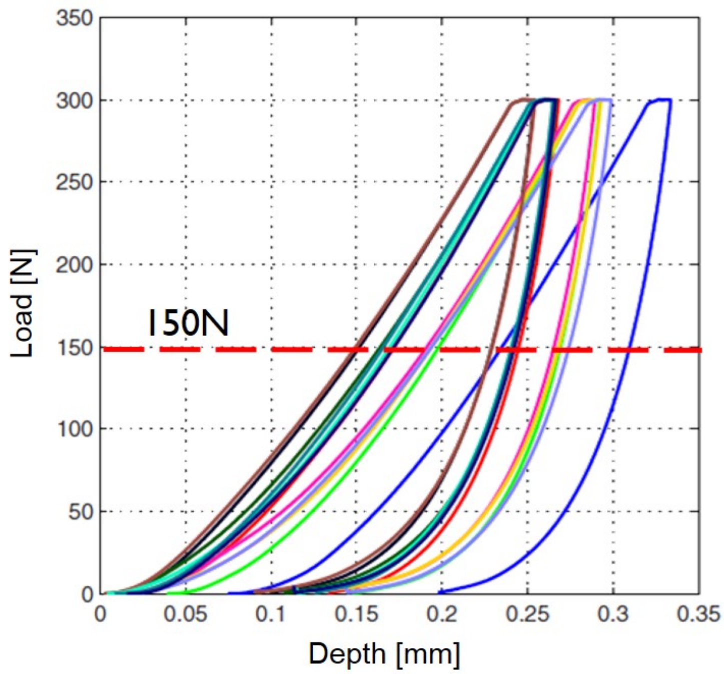

Figure 1: Indentation test on friction material on different locations

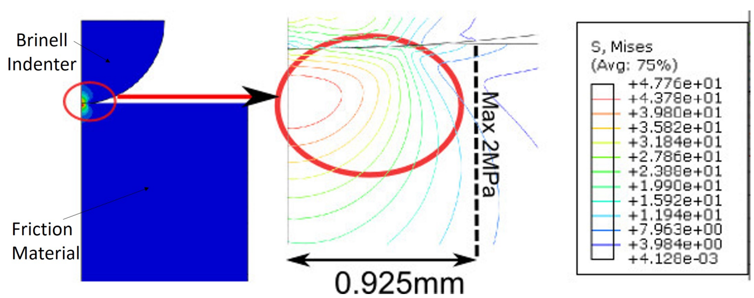

Figure 2: 2D axisymmetric model of indentation tests for definition of the mapping of the friction pad

Knowing the elementary volume affected by the indentation test ($\sim 2mm$) and taking a safety coefficient, the brake pad has been divided into 140 square areas of 5mm side (figure 3). Thus, this cutting permits to emphasize a potential heterogeneity of material behavior without impacting the surrounding.

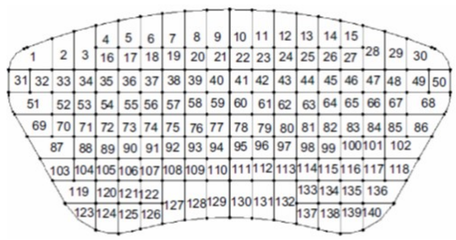

Figure 3: Mapping of the friction pad for indentation tests

3. Identification of mechanical properties via indentation test

During the two last decades, the instrumented indentation test has been developed. It allows determining some more mechanical properties of materials than the sole conventional hardness, such as Young's modulus [23], [19] [8], the work-hardening coefficient [10] [3] [14] and the yield stress [18] as well as the fracture toughness [17].
By analyzing the unloading part of a load-depth curve obtained by instrumented indentation, [23] used the following expression that relates the slope S at the origin of the unloading curve to the reduced modulus E_R:

$$E_R = \frac{S}{2}\sqrt{\frac{\pi}{A_c}} \tag{1}$$

where E_R includes the material parameters of the indenter(E_i, ν_i) and of the investigated material(E,ν) in the relation:

$$\frac{1}{E_R} = \frac{1-\nu^2}{E} + \frac{1-{\nu_i}^2}{E_i} \tag{2}$$

The difficulties with the direct use of this relation come from the inaccurate evaluation of the contact surface A_c, as when pile-up or sink-in effect at contact surface becomes important, or from the existence of a thin film which changes the apparent contact modulus at the surface. A complementary approach to the direct identification formulae is to try to extract the information about the mechanical properties directly from the load-displacement indentation curves, by making use of inverse analysis like [24]. Inverse analyses are generally based on the minimization of a cost function measuring the discrepancy between the experimental load-displacement curve and a simulated one. The loading part of the indentation measurement will be studied and exploited in the following. In fact, the loading part of the curve is the interesting part in this study because it deals with the beginning of contact and it takes into account the surface behavior which won't appear in the unloading part because it is supposed entirely volumic and elastic. Macroscopic scale indentation will be used due to the millimetric size of some raw materials. In addition, in order to study materials in specific friction states, hence not losing surface history, the samples is not prepared (no polishing or flatness / parallelism)

Nevertheless, it is necessary to remain in the elasticity domain to be sure to identify the elastic mechanical properties. In view of figure 1, a small residual deformation is present. So later, all indentation tests will be treated with a loading level below 150N.

3.1. Inverse analysis: FEMU method

Here, the objective is to found the Young Modulus in each patch by an inverse identification. Finite Element Model Updating (or FEMU) is the most widely utilized identification technique [12], [16]. It consists usually of an iterative method that relies on the comparison of the measured and computed loads and/or displacement.

The cost function θ used here aims at minimizing the gap in displacements between computations and indentation experiments. The minimization itself is done using the Levenberg-Marquardt algorithm.

$$\theta = arg\, min \sum_{i=1}^{n} (U_{fem} - U_{ind})^2 \tag{3}$$

where U_{fem} is the displacement of the indenter (as considered as rigid) in the finite element analysis and U_{ind} is the experimental displacement of the indenter. n is the number of indentation increment to go to 150N. Here, all conditions for the indentation modeling is the same as illustrated in section 2.3. The applied loading is directly deduced from the indentation tests. Two examples (on patches n^o25 and n^o50) of inverse identification are illustrated in figure 4.

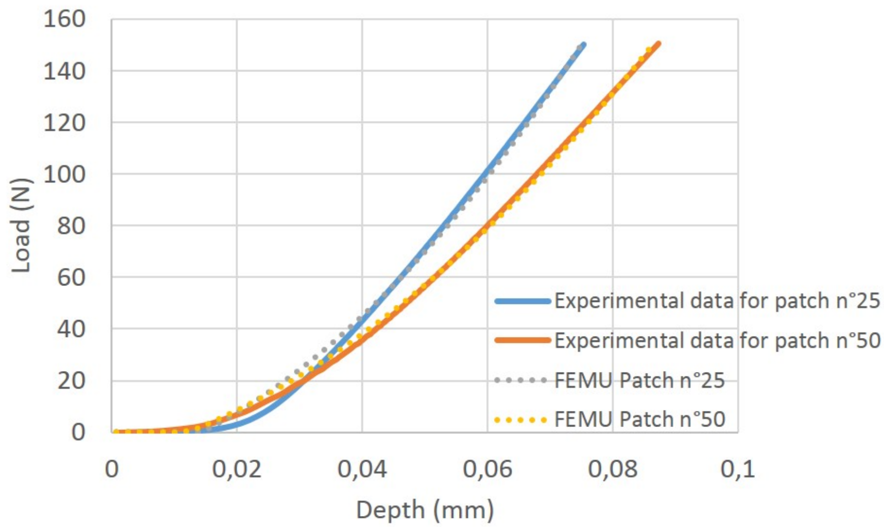

Figure 4: Inverse identification with FEMU method on patch n^o25 and n^o50

So in view of the results, the FEMU method is a good way to investigate the behavior. The tendency of the inverse method is near to the experimental data with a cumulative error less than 5%.

3.2. Braking tests

A complete investigation is done on the history effect influence through normalized test on an industrial floating caliper brake system. The procedure used in this paper is an adaptation of the SAEJ2521 procedure and is detailed further. It is a temperature-driven procedure which sweeps different pressure and velocity, dedicated mostly to determine the propensity of a given friction material to generate squeal noise on a given brake configuration, when submitted to normal or extreme temperature conditions (between room temperature to 550^{o}C). Drags and stop braking are experienced and measured. The coefficient of friction and noise frequency/level are the signatures of the brake pad. The complete procedure is composed of 2 procedures to have a longer test and to see the history effect of braking compared to SAEJ2521. The first procedure, described in figure 5, is followed by a reduced version which is stopped before fading phase (very high single braking). The procedure is repeated four times but each one is stopped at a particular moment of the procedure and withdrawn from the bench to perform an indentation test. A new pad is used for each test. The description of each test is:

- Test 1 : the test stops just before the beginning of fading phase (cycle with extreme temperature conditions). The pad won't see an elevation of initial temperature higher than 300C (at 5mm from the contact surface, into the pad center).
- Test 2 : the test stops just after the fading phase. At the end of this step, the pad has seen higher than 550C.
- Test 3 : The first procedure is done. The pad has seen 1917 brake stops, with a fading phase and some stops after.
- Test 4 : The complete procedure is done, so the pad has seen the same tasks as previous tests, with an additional procedure. The purpose is to see the effect of history and wear on mechanical properties. Maximum temperature of this additional test is around 300C.

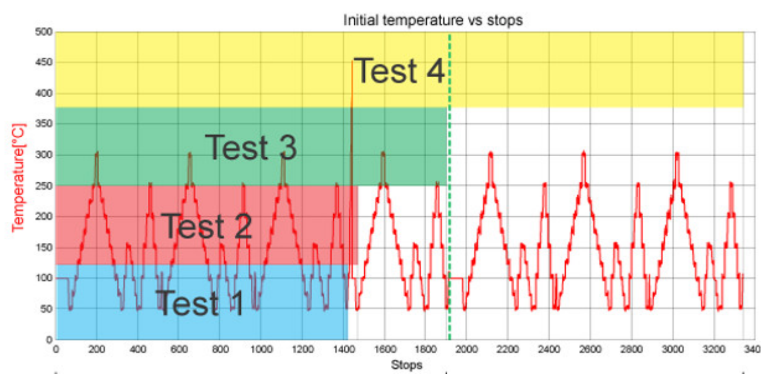

Figure 5: Test procedure description

4. Identification of local mechanical properties

4.1. Elastic modulus distribution analysis

The distribution of Young modulus is illustrated in fig. 6 using the FEMU method previously described for the different tests.

It is clear from figure 6 that the material for all tests is heterogeneous with

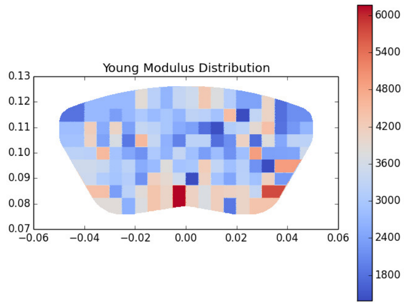

(a)

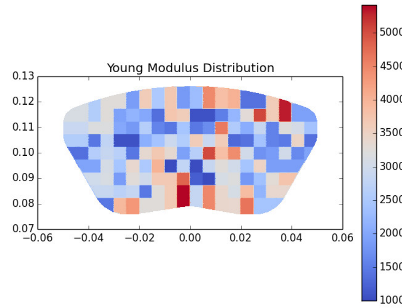

(b)

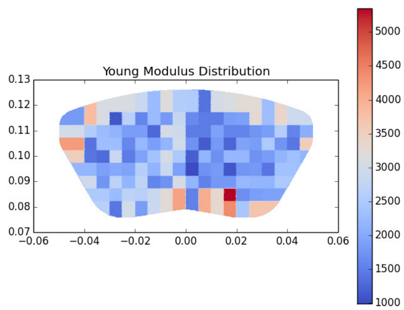

(c)

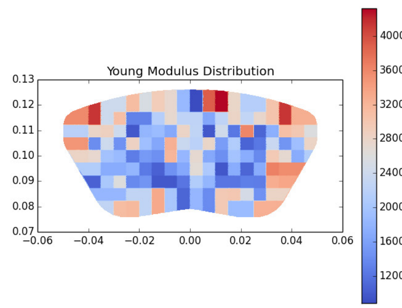

(d)

Figure 6: Young Modulus (MPa) Distribution after different tests: (a) Test 1, (b) Test 2, (c) Test 3, (d) Test 4

a range of Young modulus which is reduced in function of the history effect. Indeed, for the test 1, the range of Young modulus is from 1387 MPa to 6167 MPa while the range of Young modulus for the test 4 is 881 MPa to 4323 MPa. To see the dispersion of the Young Modulus between the different tests, the histogram 7 with a cluster of 500 MPa is presented.

A first interest is to have a global information of the bulk (equivalent) Young modulus on each pad lining. For that, a numerical compressive (fig. 8) test has been simulated using the finite element method considering the heterogeneity of the modulus previously identified.

Considering a displacement x on the upper surface and a blocking displacement on the below surface, the reaction F can be obtained. The equiv-

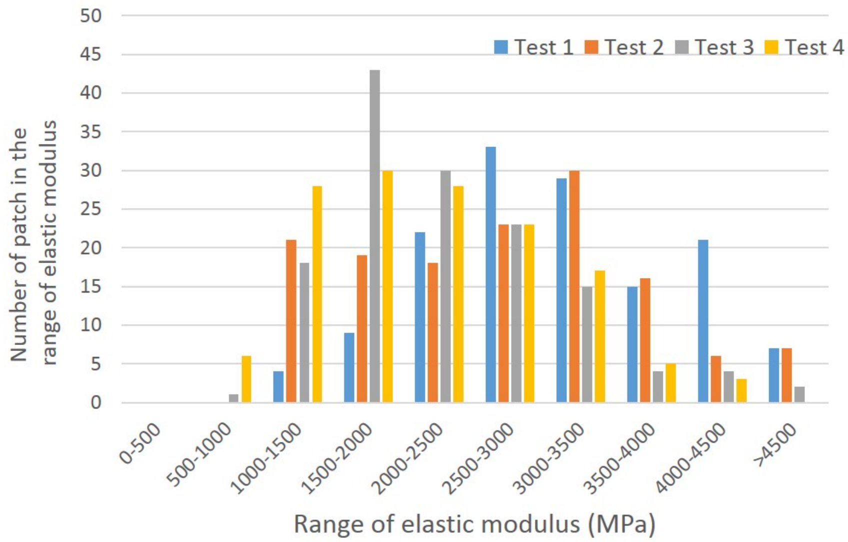

Figure 7: Cluster of elastic modulus per sliding state

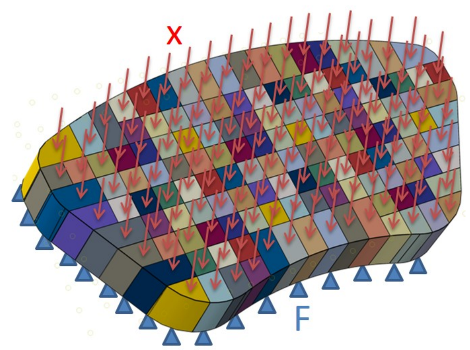

Figure 8: Procedure to obtain equivalent Young modulus

alent Young modulus E_{eq} is finding using:

$$E_{eq} = F * L/x * A \tag{4}$$

with F: Reaction, L:Width of material, x: imposed displacement and A: Pad surface area.

Table 4.1 shows the evolution of the equivalent Young modulus for all tests, exhibiting a significant decrease between test 1 and 2, only different with one intense braking and between test 2 and 3.

	Test 1	Test 2	Test 3	Test 4
E_{eq}	3240 MPa	2872 MPa	2464 MPa	2368 MPa

Table 1: History effect on the Equivalent Young Modulus (E_{eq})

To conclude, the friction materials present a certain heterogeneity for all the tests. The range of heterogeneity decrease in function of the history effect and the equivalent Young modulus decrease also.
This evolution of the Young modulus can be associated with a modification of the microstructure where the thermal effect has a great influence on the mechanical properties [9].

A remark can be made about the distribution of the Young modulus for all the tests: the average of Young modulus localized at the periphery patch is stiffer than the ones localized on the pad inner surface. Table 4.1 shows the average value for each region (periphery and inside) and the associated standard deviation for each case.

	Test 1	Test 2	Test 3	Test 4
E_{per} MPa *(standard deviation MPa)*	3309*(844)*	2932*(990)*	2800*(894)*	2446*(836)*
E_{in} MPa *(standard deviation MPa)*	3053*(856)*	2634*(994)*	2062*(563)*	2084*(732)*

Table 2: E_{per}: Average of Young modulus localized at the periphery patch and E_{in}: Average of Young modulus of inside patches

For each test, the average Young modulus localized at the periphery is clearly stiffer than the average Young modulus of inside pad with a global difference of $\sim$400MPa. The authors think that this result can be due to the manufacturing process. Indeed, the friction lining is mold and a uniaxial pressure is applied on the upper surface. So the border effect with the mold must densify the material localized at the periphery.

5. Brake squeal analysis

The previous section has supplied a methodology to estimate local heterogeneities mechanical properties of the pad. Here, the target is to implement these properties into a numerical simulation of brake squeal propensity. The effect and contribution of each configuration with heterogeneity (called hete. $N^o i$ latter) and its equivalent homogeneous case (called homo. $N^o i$ latter) are discussed. A complex eigenvalue analysis considering a complete brake system is used in order to draw attention to the key role of the heterogeneities and its evolution on mode lock-in. Patches on the pad volume are distributed according to indentation mapping as introduced in section 3.

5.1. Description of the numerical model

A finite element model (fig. 9) of a complete automotive brake corner was created on Abaqus 13.0. The system, shown in figure 9, consists in a vented disc, a brake system (fixed calipers, pistons, pins and lining) and a front axle system (anchor, knuckle). The model is made of 232,913 solid elements with first-order (linear).
All materials are considered as isotropic in this model. The disc is a grey cast-iron disc with an elastic modulus of 118GPa, a Poisson ratio of 0.25 and density of $7200kg/m^3$. The density of the friction pad is fixed to $2480kg/m^3$. The pad backplate Young modulus is equal to 210GPa and other components have a Young modulus at 172GPa.
Coefficient of friction between pad and disc is equal to 0.4. Both linings properties are considered as symmetric in this simulation extracting from the indentation identification previously described.

Figure 10 illustrates an overview of all contacts (C_i with $i = 1..7$ for contact and T for tied conditions) between the different components. A tied condition is applied between the pins and the caliper and between each backplate and the associated friction material. The other contacts are modeled using Augmented Lagrange methods in the normal direction and using Penalty method in the tangential direction. Surface-to-surface formulation and small sliding conditions are adopted. Only the pad-to-disc interface is modeled using the node-to-surface formulation and the small sliding condition.

A pressure of 1 MPa on the pistons (blue region in figure 11(b)) is applied and the following boundary conditions are applied:

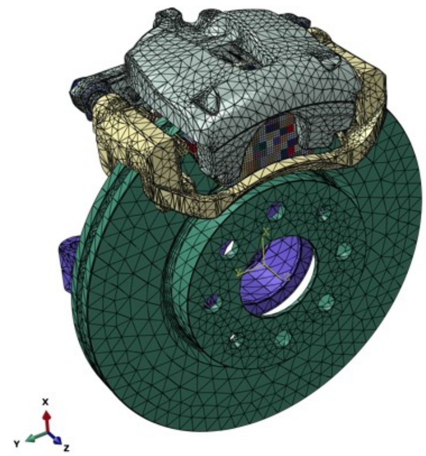

Figure 9: Finite element model of the automotive brake corner.

- On the surface with the label 1 on figure 11(a), all displacements are fixed
- On the surface with the label 2 on figure 11(a), only axial displacement is fixed
- On the surface with the label 2 on figure 11(a), all displacements except the axial one are fixed

Moreover, a rotation of disk is applied $5rad.s^{-1}$ like illustrated in figure 11(b) by a yellow arrow.

5.2. Results

5.2.1. Quasi-static results

In this section, the results of the mechanical analysis after the rotation step are presented for homogeneous and heterogeneous friction pad material for configuration 1. Contact pressure is shown at pad interfaces in figure 12 for inner and outer pads. Contact covers all both pads from leading to trailing edge. Due to the difference of the loading application, the pressure distribution is different between the inner friction pad and the outer one.

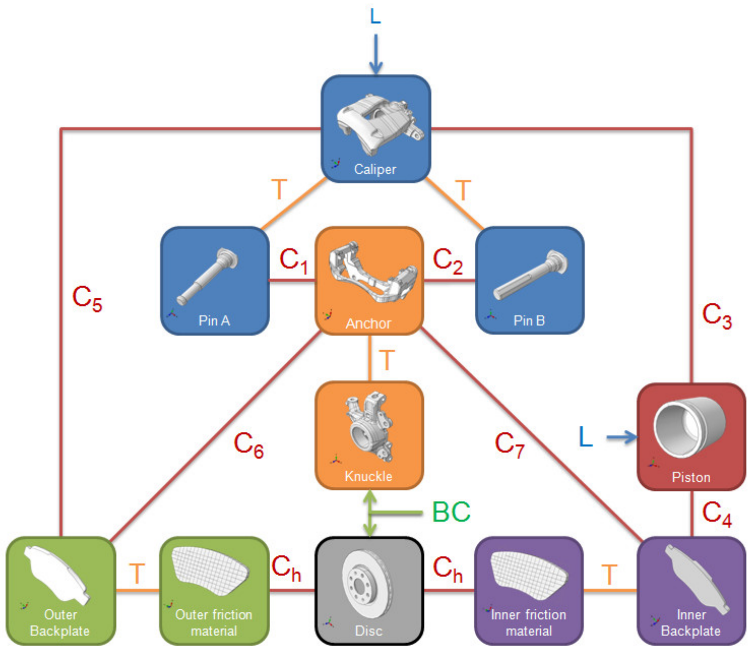

Figure 10: Summary of all interactions in the model

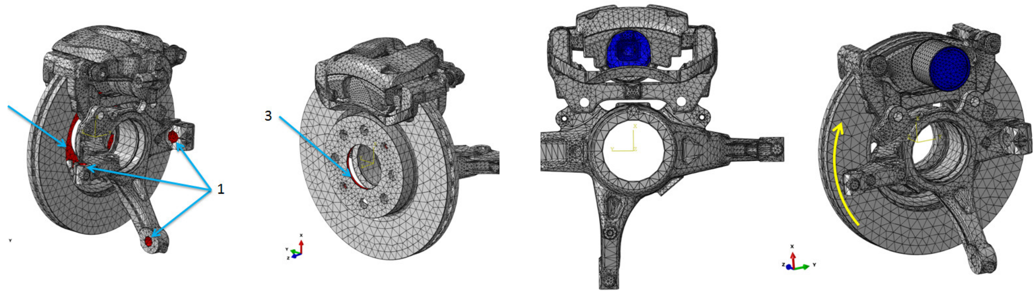

(a) (b)

Figure 11: Boundary conditions on the brake system model: (a) Boundary Conditions, (b) Loading

Nevertheless, for the heterogeneous case, the pressure is more localized at more stiffer patches.

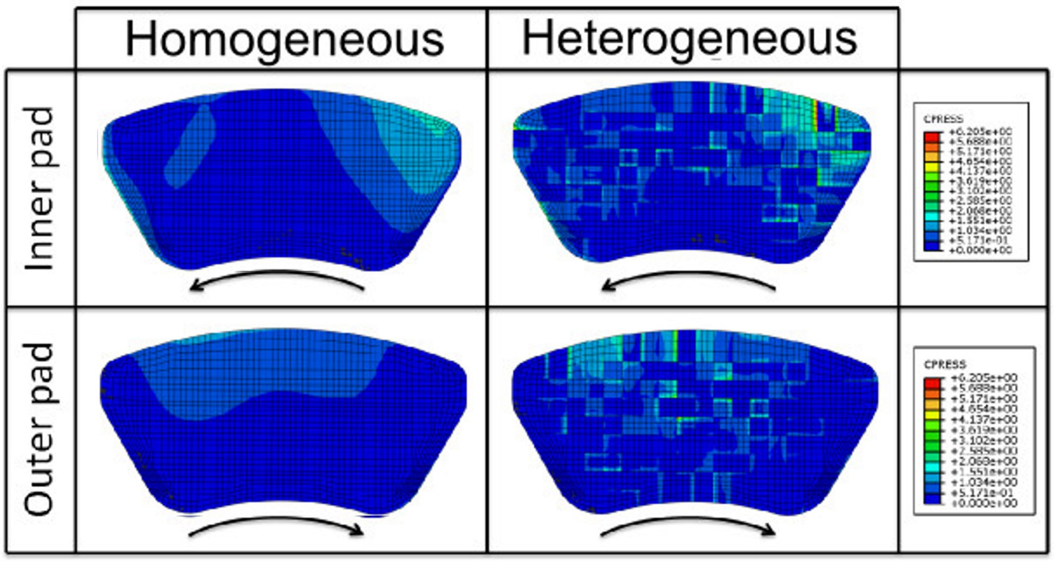

Figure 12: Pressure distribution of homogeneous and heterogeneous cases for the configuration 1

5.2.2. Complex modal analysis results: Homogeneous vs. Heterogeneous configurations

The complex eigenvalues analysis is summarized in table 5.2.2 and only eigenfrequencies with a real part different of zero are reported according to the deformed shape. Firstly, the comparison is performed considering the heterogeneous identified on the test N^o1 and the associated homogenized (taking into consideration an effective Young modulus).

The results show that more unstable cases occur in the heterogeneous configurations in the frequencies range of [0, 8000Hz]. Another observation validated for all configurations comparing homogenized and heterogeneous configurations show that the unstable cases of the homogenized configuration are systematically found in the heterogeneous cases. The opposite is not true.

Deformed shape	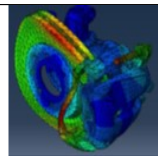 N^o1	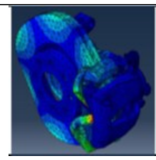 N^o2	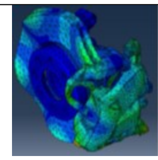 N^o3	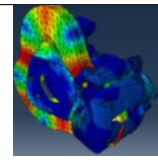 N^o4	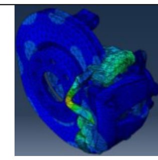 N^o6
Homo. 1		3128 Hz			7930 Hz
Hete. 1	1900 Hz	3120 Hz	6303 Hz	6685 Hz	7893 Hz

Table 3: Eigenfrequencies (with a non zero real part) and eigenmodes for heterogeneous and homogenized of configuration 1

5.2.3. Complex modal analysis results: Heterogeneous configurations

Results of the complex eigenvalues analysis are summarized in table 5.2.3 and only eigenfrequencies with a real part different of zero are reported.

Deformed shape	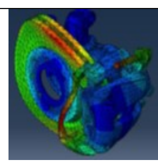 N^o1	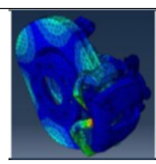 N^o2	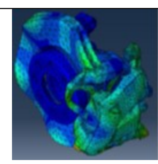 N^o3	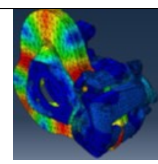 N^o4	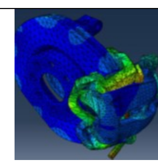 N^o5	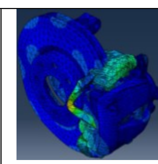 N^o6
Hete. 1	1900 Hz	3120 Hz	6303 Hz	6685 Hz		7893 Hz
Hete. 2		3115 Hz				7817 Hz
Hete. 3		3111 Hz	6286 Hz	6684 Hz	7566 Hz	7779 Hz
Hete. 4	1974 Hz	3112 Hz			7573 Hz	7752 Hz

Table 4: Eigenfrequencies (with a non zero real part) and eigenmodes for different configurations

First of all, eigenmodes N^o2 and N^o6 are always present for all pad material configurations as far as for the homogenized case. Indeed, these eigenmodes correspond to global system deformation with quasi any-influence of the friction material properties.
In the same way, the eigenmode N^o5 corresponds to a global system dynamic behavior appearing above a certain value of the equivalent friction material modulus and the heterogeneity does not have an effect on this mode lock-in. For the remaining eigenmodes (n 1-3-4), heterogeneity has a significant impact.

6. Conclusions

An original approach for friction material characterization has been developed based on a dialogue of experimental and numerical methods. Indeed, the material behavior has been modeled with an indentation static simulation from experimental tests. A material behavior model has been built from the stress-strain response. Using an inverse identification, the implementation of the elastic parameters gives a satisfactory equivalent to the experimental test. On a complete brake pad, this methodology improves the existing method of enriching material volumic properties, associated with distributed properties on the pad surface. For each pad, the identification has been done with 140 imprints that have been introduced in the numerical model on 140 patches of the surface. Another aspect broached is to work at different friction pad states. Indeed, four pad stopped at different friction states are studied. Identification of material behavior model shows that the heterogeneity is very strong at different friction states with a global decrease of the equivalent bulk Young Modulus depending on the history effect. This history effect has an impact on the roughness too which changes the local stiffness as shown by [13]. A complete model considering the floating caliper and vented disc as in real test application, coupled with data acquired with indentation have been studied in a complex eigenvalue analysis. Numerical contact and eigenvalue analysis show that the heterogeneity or the equivalent homogenized behavior can have a strong influence on the results (contact pressure distribution and unstable frequencies). In the following, the numerical results will be compared to experimental ones.

Acknowledgments

The present research work has been supported by the international Campus on Safety and Intermodality in Transportation, the Nord-Pas-de-Calais Region, the European Community, the Regional Delegation for Research and Technology, the Ministry of Higher Education and Research, and the National Center for Scientific Research. The authors gratefully acknowledge the support of these institutions. The investigations and results reported herein are supported by the National Research Agency (France) under the COMATCO research program.

References

[1] Abubakar, A. and Ouyang, H. (2006). *Complex eigenvalue analysis and dynamic transient analysis in predicting disc brake squeal.*, International Journal of Vehicle Noise and Vibration, 2(2):143155.

[2] Akay, A., 2002. *Acoustics of friction*, J. Acoust. Soc. Am., Vol. 111, No. 4.

[3] Antunes, JM., Fernandes, JV., Menezes, LF., Chaparro, BM.(2007) *An new approach for reverse analyses in depth-sensing indentation using numerical simulation.* Acta Mater;55:6981.

[4] Baba H., W. T. and Takagi, T. (2001). *Study on reduction of brake squeal caused by in-plane vibration of rotor.*, SAE Paper 2001-01-3158.

[5] Bae, J. C. and Wickert, J. A. (2000). *Free vibration of coupled diskhat structures.* Journal of Sound and Vibration, 235(1):117132.

[6] Bergmann, F., Eriksson, M., and Jacobson, S. (2000). *The effect of reduced contact area on the occurence of disc brake squeals for automotive brake pad.*, Proceeding of the Institution of Mechanical Egineers, D 214 (D5):561568.

[7] Bigerelle, M., Nianga, J.M., Najjar, D, Iost, A., Hubert, C. and Kubiak, KJ. (2006). *Roughness signature of tribological contact calculated by a new method of peaks curvature radius estimation on fractal surface.*, Tribology International, 65:235-247.

[8] Chicot, D.,deBaets, P., Staia, MH.,Puchi-Cabrera, ES.,Louis, G.,Perez-Delgado, Y., 2013. *Influence of tip defect and indenter shape on the mechanical properties determination by indentation of a TiB260% B4C ceramic composite.* Inter J Refract Met Hard Mater;38:10210.

[9] Cristol, A.L., Magnier, V. 2015. *Impact of braking on microstructure and mechanical properties of friction material*, Conf. Eurobrake 2015, Dresden, Deutschland .

[10] Dao, M.,Chollacoop, N.,Van Vliet, KJ., Venkuatesh, TA., Suresh, S. (2001). *Computational modeling of the forward and reverse problems in instrumented sharp indentation.* Acta Mater ;49:3899918.

[11] Duboc M., 2013. *Etude multiéchelle du crissement : dispositif expérimental et éléments de compréhension*, PhD Thesis, Université de Lille 1.

[12] Hermez, F., Farhat, C. (1993). *Updating finite element dynamic models using element-by-element sensitivity methodology.* AIAA J 31(9):17021711

[13] Heussaff, a., Dubar, L., Tison, T., Watremez, M., and Nunes, R. (2012). *A methodology for the modelling of the variability of brake lining surfaces.*, Wear, 289:145159.

[14] Huber, N, Tsakmakis, Ch. (1999).*Determination of constitutive properties from spherical indentation data using neural networks. PartI:the case of pure kinematic hardening in plasticity laws.*J Mech Phys Solids, 47:156988.

[15] Guan, D. and Jiang, D. (1998). *A study on disc brake squeal using finite element methods.* SAE Paper 980597.

[16] Kavanagh, K., Clough, R. (1971). *Finite element applications in the characterization of elastic solids.* Int. J. Solids Struct 7:1123

[17] Kruzic, JJ., Kim, DK.,Koester, KJ., Ritchie, RO. (2009). *Indentation techniques for evaluating the fracture toughness of biomaterials and hard tissues.* JMechBehavBiomedMater;2:38495.

[18] Kucharski, S.,Mroz, Z. (2007). *Identification of yield stress and plastic hardening parameters from a spherical indentation test.* IntJMechSci;49:123850.

[19] Loubet, JL.,Bauer, M.,Tonck A., Bec S.,Gauthier, B. *Mechanical properties and deformation behaviour of material shaving ultra-fine microstructures.* NATOAS;233:42947.

[20] Nagy, L., Cheng, J., and Hu, Y. (1994). *A new method development to predict squeal occurrence.*, SAE Paper 942258.

[21] Magnier, V., Roubin, E., Colliat, J.B. and Dufrnoy, P. (2017). *Methodology of porosity modeling for friction pad: Consequence on squeal*, Tribology International, 109:78:85.

[22] Naidoo Ramasami, D. (2014). *Influence of friction material and test sequence on disc brake squeal*, PhD Thesis, Université de Lille 1.

[23] Oliver, WC., Pharr, GM. (1992). *An improved technique for determining hardness and elastic modulus using load and displacement sensing indentation experiments.* JMaterRes ;7(6):156483.

[24] Prou, J., Kishimoto, K., Constantinescu, A. (2010). *Identification of Young's Modulus from Indentation Testing and Inverse Analysis.* Journal of Solid Mechanics and Materials Engineering; 4(6):781-795.

[25] Shi T.S., C. W. K. D. O. J. A. M. and Warzecha, T. (2001). *Advances in complex eigenvalue analysis for brake noise.* SAE Paper 2001-01-1603.

[26] Waddad, Y., Magnier, V., Dufrénoy, P. and De Saxceé, G. (2016). *A multiscale method for frictionless contact mechanics of rough surfaces.*, Tribology International, 96:109-121.

[27] Yang, M. and Afeneh, A.-H. (2004). *Investigation of mounted disc brake in-plane and out-of-plane modes in brake squeal study.*, Experimental Mechanics, S., editor, Proceedings of the 22nd Int. Modal Analysis Conference (CD-ROM).